A Microwave Engineering Perspective of the Superlens

Ravi S. Hegde, Yew Li Hor, and Wolfgang J. R. Hoefer*

Institute of High Performance Computing, A-Star, Singapore
*corresponding author, E-mail: hoeferwjr@ihpc.a-star.edu.sg

Abstract

Super-resolution imaging involves the interaction of electromagnetic waves with objects that have dimensions similar to, or smaller than the wavelength. That is precisely the hallmark of microwave technology. It suggests that microwave concepts and design approaches may not only be helpful in the description and modeling of the superlens behavior, but also provide useful tools for designing and realizing the superlens, notably the metamaterial itself. In this paper we present some interesting results and insights yielded by the microwave perspective, including waveguide, circuit and filter representations of the superlens.

1. Introduction

The goal of modeling devices or physical processes is to capture their essential characteristics. Reduction to the simplest possible representation not only facilitates their theoretical and numerical treatment but also can provide insights that are helpful in relating new observations to known phenomena. In the case of superresolution imaging with the Veselago/Pendry superlens [1][2] consisting of double-negative metamaterial, the use of waveguide and lumped element circuit models can considerably simplify both its theoretical and its numerical analysis at various levels of abstraction[3]. Given the long time required for the lens to reach the steady-state [4][5][6][7], such simplified models facilitate exploration of resolution limits, allow easy quantification of its imaging performance, and provide a link to microwave engineering and filter design. In this paper we highlight some interesting results and insights yielded by the microwave and filter perspective [6].

2. Waveguide model of sub-wavelength imaging

The imaging of a sub-wavelength sized object is typically based on a spatial Fourier transform of the field emanating from the object, either directly or by scattering of an incident field. The resulting continuous spatial spectrum is then transferred in the frequency domain through the superlens, and the image is recovered by inverse Fourier transform. In the general case this is a three-dimensional electromagnetic problem that must be solved in a semi-infinite half-space. Clearly, the treatment of this problem with space- and time-discrete numerical methods such as FDTD or TLM [8], will require large computational resources and long simulation times.

2.1. Discretization of the spatial spectrum

The first major simplification of the problem is achieved by discretizing the spatial spectrum of the object field into a series of harmonically related samples. This yields a spatial Fourier series; its inverse Fourier transform corresponds to the field produced not by a single object, but by an infinite array of such objects. Fig. 1 illustrates this concept for an object field that has the form of a half-cosine (approximating the field in a narrow slot illuminated by a plane wave polarized parallel to the slot (Fig. 1a)). The spatial Fourier transform perpendicular to the slot is given by:

$$F(k) = \frac{2w/\pi}{1-k^2(w/\pi)^2}\cos(kw/2) \quad , \qquad (1)$$

where w is the width of the slot, and $k=2\pi/\lambda_t$ is the transverse wavenumber or spatial angular frequency. (1) represents the continuous spatial spectrum shown in normalized form in Fig. 1b. If we sample this spectrum at intervals $n=k/\Delta k$ we obtain a Fourier series which represents the discrete spectrum of an infinite array of identical slots separated by a distance $s=2\pi/\Delta k$ (the red curve in Fig. 1a).

The latter curve has been obtained by adding only the first six Fourier terms together. Again, the functions are normalized for better comparison. This example shows that the image of a single slot is well approximated by an image of periodic slots over the base w. However, the discrete Fourier series approximation considerably simplifies the mathematical formulation of image transmission by the superlens. It naturally leads to the spectral waveguide model of the superlens reported in [6]. This model not only yields existing steady-state formulations of superlens behavior in well-known waveguide terminology, but it also dramatically reduces the computational burden of numerical solutions when studying the dynamics of the lens. Note that this waveguide model describes the transfer of the object field to the image plane in terms of propagating and evanescent waveguide modes and is not a representation of the metamaterial of the lens. It is especially helpful in the transient numerical analysis of superlens behavior that requires millions of time steps [6].

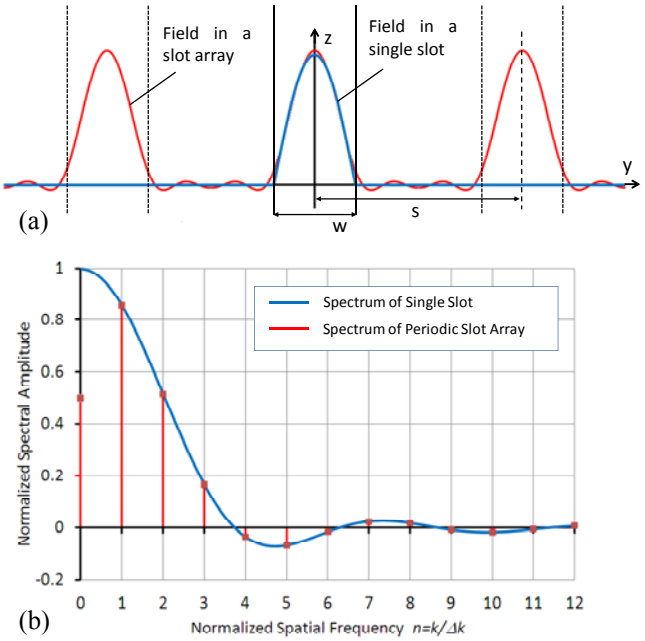

Fig. 1 (a) Electric field in a single slot and in periodic slots in a perfect conductor. (b) Normalized spatial spectrum of the single slot (continuous) and of periodic slots (discrete). *w=40 nm, s=100 nm.* Note that the term at *n=0* has only one-half the amplitude of the continuous spectrum since the spectral terms for negative *n* are not included in the discrete spectrum.

2.2. Waveguide model of coupled plasmonic resonances

The spectral waveguide model is well suited for the investigation of the dynamic field response of the superlens. As discussed in [4][5][9][10][11] the evanescent part of the object field (transmitted in the form of evanescent waveguide modes) excites surface resonances on the two faces of the superlens, thus forming a system of two weakly coupled resonators. In fact, the lens can support an even and an odd mode of coupled resonances. Their resonance frequencies are the roots of a transcendental transmission line equation formulated in terms of waveguide impedances and propagation constants. The equivalent transmission line models are shown in Fig. 2. When we simulate the metamaterial lens in the waveguide model using the time domain TLM method, we employ a dynamic double-Drude model that allows the metamaterial parameters to evolve naturally with time and frequency during the transient build-up of electromagnetic energy in the metamaterial. Its parameters ε' and μ' are given in [6], and the TLM implementation of the Drude model is derived in [8]. Note that in this model ε' and μ' have the same frequency dependence. Hence, only the refractive index changes while the intrinsic impedance remains constant. The propagating part of the object field will thus cross the lens without scattering at the lens interfaces, even when the frequency deviates from the operating frequency. For TE excitation as in Fig. 1(a), all evanescent modes exhibit inductive behavior in the air-filled waveguide sections, while they behave capacitively in the metamaterial section. This indicates that the resonant response of the lens can be predicted by an extremely simple lumped element network consisting of two resonant LC circuits that are loosely coupled through a small reactive series element. This opens the way to the application of circuit and filter concepts to superresolution imaging.

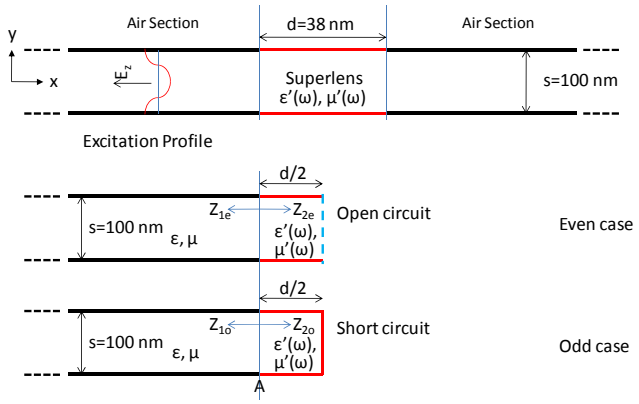

Fig. 2 Odd and even resonance conditions of the metamaterial superlens, modeled by the equivalent waveguide model. Even and odd eigenfrequencies are those frequencies at which the sum of the two impedances Z_{1e} and Z_{1o} in the plane *A* becomes zero in the even and odd cases, respectively (after [6]). The double-Drude frequency dependence of ε' and μ' is included in the transcendental resonance conditions.

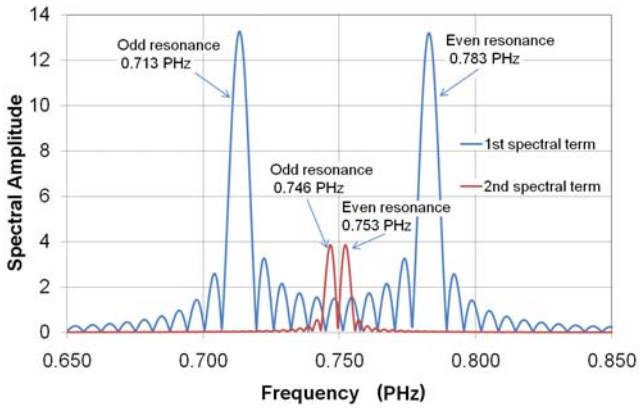

Fig. 3 Even and odd eigenfrequencies of the superlens for transverse wavelengths of *100 nm* (first spectral term) and *50 nm* (second spectral term), obtained with MEFiSTo-3D Pro simulation. Simulation data and theoretical values predicted by the transverse resonance conditions in Fig. 2 agree within *0.1%* (From [6] © 2011 IEEE).

3. Lumped equivalent circuit of the superlens

The equivalent circuit of the lens and its even and odd variants that emulate the responses of the lens at the operating frequency and at the even and odd frequencies are shown in Fig. 4 a-c. The waveguide formalism yields

simple expressions for the elements of the equivalent circuit in terms of the wave properties of the metamaterial at ω_0 [6]. However, to accurately predict the even and odd resonant frequencies the capacitive elements of the circuit model should ideally be frequency-dependent. This would complicate the circuit model, and since the lens is used essentially at the operating frequency ω_0, it is more important to accurately predict the field transmission at ω_0 then the even and odd resonant frequencies. In fact, the error in the circuit prediction becomes negligible for higher-order spectral terms where the coupling across the lens weakens exponentially until the two resonances degenerate onto a single resonance at ω_0. This tendency is clearly visible in Fig. 3.

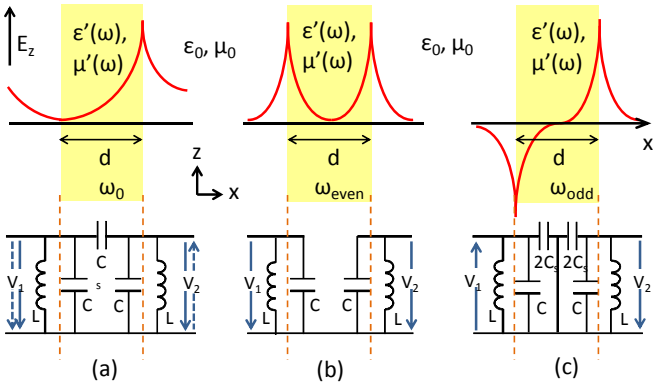

Fig. 4 Electric field distribution and equivalent lumped element circuit of an evanescent mode in the superlens (a) at the operating frequency, (b) at the even, and (c) at the odd frequency of resonance.

Note that the models in Figs. 2 and 4 are valid for individual evanescent spectral terms, but the values of the circuit elements are different for different spectral terms.

The final step is now to create an equivalent network representation of an entire superresolution system based on a perfect Veselago/Pendry lens. Such a network includes a simple transmission line section for the propagating part of the spectrum, and one equivalent circuit for each evanescent term. Knowing that at the operating frequency the field decays exponentially in positive x-direction, each section can be represented by an ideal transformer of turn ratio $n_1 = e^{k_{xn}d/2}$ where k_{nx} is the longitudinal decay constant of the *n-th* spectral term. This value is based on the assumption that the object and image planes are both located at a distance $d/2$ on each side of the lens. The network thus consists of as many modal equivalent networks as there are Fourier terms to be transmitted (see Fig. 5).

The steps involved in the image transmission with this model are as follows:

a. Perform a spatial Fourier transform of the object field produced by the sub-wavelength object;
b. Discretize the spectrum into a Fourier series;
c. Determine the parameters of the equivalent circuit in Fig. 5 for each evanescent Fourier term (details are given in [15];
d. Compute the output voltage of each circuit in response to the excitation by the appropriate Fourier term (Voltage proportional to the Fourier coefficient);
e. Compose the image by combining all transmitted Fourier terms with their appropriate structure function.

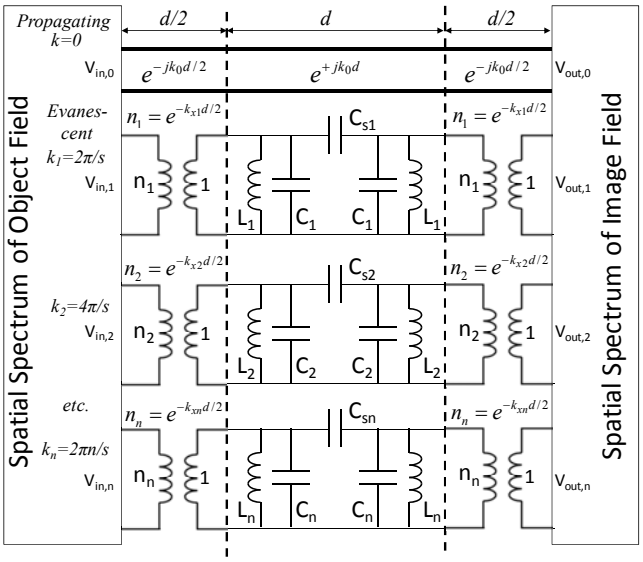

Fig. 5 Equivalent network for predicting the transmission of the discrete spatial Fourier spectrum of an object through a double-negative superlens. The system comprises one set of transmission lines for the propagating term and one coupled resonator pair for every evanescent term of the discrete spatial spectrum. V_{in} and V_{out} correspond to the modal amplitudes of the E-field in the object and image planes.

One might ask what the benefit of such an equivalent circuit would be when there exists already a well-known analytical transfer function in the literature that will give the same result. The main advantage of the circuit model is the physical interpretation of the lens as a system of two coupled resonators [6] [7] which could be used as a technology for alternative superresolution structures [12][13]. The fishnet concept, for example, employs coupled resonant apertures that can be represented by circuit models [14] very similar to our coupled resonator model in Fig. 5. The challenge is to create coupled resonating structures that are small enough to resolve the spatial wavelength of the highest term of the spatial Fourier spectrum in the transverse plane. For the dimensions given in Fig. 2 a maximum of five terms $(0 \le n \le 4)$ can typically be transmitted by the lens [6]. Fig. 11 of [6] shows typical images of a sub-wavelength slot, obtained by adding four and five transmitted Fourier terms together. Further research is underway to explore how to realize and arrange

the different modal resonators to achieve sufficiently large spatial bandwidth suitable for superresolution imaging.

4. Conclusions

We have shown that the field emitted or scattered by a sub-wavelength object can be closely approximated by a Fourier series through sampling of its continuous spectrum. The discrete spectral terms can be interpreted as the eigenmodes of a spectral waveguide model that allows us to describe the superlens imaging of the object using waveguide formalism. The waveguide model is especially useful for numerical modeling of superlens imaging because it provides a compact computational domain truncated by boundary conditions that are numerically robust (perfect electric and magnetic walls), and allows fine discretization and large numbers of time steps that are required to handle the long settling times of the higher evanescent spectral terms. The waveguide model naturally leads to an even simpler coupled resonator model of the Veselago-Pendry superlens which provides deeper physical insight into the physics of the superlens, connects it with the theory of filters and resonant surfaces, and may facilitate the search for alternative ways to realize superresolution devices.

Acknowledgements

This work was supported by the Government of Singapore's Science and Engineering Research Council through A*Star SERC Grant No. 092 154 099 titled "Metamaterials Programme: Superlens".

References

[1] Veselago, V.G., "The electrodynamics of substances with simultaneously negative values of ε and μ," Sov. Phys. Usp., vol. 10, no. 4, pp. 509–514, Jan.-Feb. 1968.

[2] Pendry, J. B. "Negative refraction makes a perfect lens" *Phys. Rev. Lett*., vol. 85, no. 18, pp. 3966–3969, Oct. 2000.

[3] L. Solymar and E. Shamonina, *Waves in Metamaterials,* New York: Oxford University Press, 2009, pp. 157-159.

[4] G. Gomez-Santos, "Universal features of the time evolution of evanescent modes in a left-handed perfect lens" *Phys. Rev. Lett.,* vol. 90, no.7, pp. 077401-1 – 077401-4, Feb. 2003.

[5] X. S. Rao and C. K. Ong, "Subwavelength imaging by a left-handed material superlens", Phys. Rev. E, vol. 68, pp. 067601-1 – 067601-3, Dec. 2003.

[6] Hegde, R.S., Zs. Szabó, Y.L. Hor, Y. Kiasat, E.P. Li and W.J.R. Hoefer, "The Dynamics of Nanoscale Superresolution Imaging with the Superlens" IEEE Trans. Microw. Theory Tech., vol. 59, no. 10, pp. 2612-2623, Oct. 2011.

[7] . H. Wee, J. B. Pendry, "Universal Evolution of Perfect Lenses," Phys. Rev. Lett. 106, 165503 (2011).

[8] P. P. M. So, H. Du and W. J. R. Hoefer, "Modeling of metamaterials with negative refractive index using 2-D shunt and 3-D SCN TLM networks", *IEEE Trans. Microw. Theory Tech*., vol. 53, no. 4, pp. 1496–1505, Apr. 2005.

[9] R. Ruppin, "Surface polariton of the left-handed medium," *Phys. Lett. A*, vol. 277, pp. 61-64, 2000.

[10] F. D. M. Haldane, "Electromagnetic surface modes at interface with negative refractive index make a 'not-quite-perfect' lens," *Cond. Matt.,* 0206420, 2002.

[11] D. L. Sounas, N. V. Kantartzis, and T. D. Tsiboukis, "Temporal characteristics of resonant surface polaritons in superlensing planar double-negative slabs: Development of analytical schemes and numerical models," *Phys. Rev.* E 76, 046606-1-046606-12, 2007.

[12] A. Alu, N. Engheta, "Pairing an epsilon-negative slab with a mu-negative slab: resonance, tunneling and transparency," *IEEE Transactions on Antennas and Propagation*, vol. 51, issue 10, pp. 2558-2571, 2003.

[13] A. Alu, N. Engheta, "Distributed-circuit-element description of guided-wave structures and cavities involving double-negative or single-negative media," in *Proc. SPIE* 5218, 145 (2003).

[14] R. Marquès, L. Jelinek, F. Mesa, and F. Medina, "Analytical theory of wave propagation through stacked fishnet metamaterials," *Optics Express*, vol. 17, no. 14 /, 11582, 2009.

[15] W. J. R. Hoefer, "The Superlens as a Filter of the Spatial Spectrum" *in 2012 IEEE MTT_S International Microwave Symposium Dig.*, paper WE3H-10, Montreal, Canada, Jun. 17-22, 2012.